Bioactive Materials 6 (2021) 146–157

Contents lists available at ScienceDirect

Bioactive Materials

journal homepage: http://www.keaipublishing.com/biomat

# Regulation of the inflammatory cycle by a controllable release hydrogel for eliminating postoperative inflammation after discectomy

Yu Liu[a,1], Jiacheng Du[a,1], Peng Peng[a,1], Ruoyu Cheng[b], Jiayi Lin[a], Congxin Xu[a], Huilin Yang[a], Wenguo Cui[b], Haiqing Mao[a,**], Yuling Li[b,c,*], Dechun Geng[a,***]

[a] Department of Orthopaedics, The First Affiliated Hospital of Soochow University, Suzhou, Jiangsu, 215006, PR China
[b] Shanghai Institute of Traumatology and Orthopaedics, Shanghai Key Laboratory for Prevention and Treatment of Bone and Joint Diseases, Ruijin Hospital, Shanghai Jiao Tong University School of Medicine, 197 Ruijin Second Road, Shanghai, 200025, PR China
[c] Department of Orthopaedics, Affiliated Hospital of North Sichuan Medical College, No.63 Wenhua Road, Nanchong, Sichuan, 637000, PR China

ARTICLE INFO

*Keywords:*
Composite hydrogel
Intervertebral disc degeneration
Recurrence
Inflammation
Aspirin

ABSTRACT

Surgery is the final choice for most patients with intervertebral disc degeneration (IDD). Operation-caused trauma will cause inflammation in the intervertebral disc. Serious inflammation will cause tissue defects and induce tissue degeneration, IDD recurrence and the occurrence of other diseases. Therefore, we proposed a scheme to treat recurrence after discectomy by inhibiting inflammation with an aspirin (ASP)-loaded hydrogel to restore the mechanical stability of the spine and relieve local inflammation. ASP-liposomes (ASP-Lips) were incorporated into a photocrosslinkable gelatin-methacryloyl (GelMA) via mixing. This material can effectively alleviate inflammation by inhibiting the release of high mobility group box 1 (HMGB1) from the nucleus to the cytoplasm. We further assessed the expression of inflammatory cytokines, such as interleukin 6 (IL-6) and tumor necrosis factor-α (TNF-α), and degeneration-related factors, such as type II collagen (COL-2), Aggrecan, matrix metallopeptidases-3 (MMP-3), MMP-13, a disintegrin and metalloproteinase with thrombospondin motifs-4 (ADAMTS-4) and ADAMTS-5 in rat nucleus pulpous cells. The level of IDD was analyzed through H&E, safranin-O staining and immunohistochemistry in rabbit samples. *In vitro*, we found that ASP-Lip@GelMA treatment significantly decreased inflammatory cytokines, MMP-3 and -13, and ADAMTS-4 and -5 and up-regulated COL-2 and Aggrecan via the inhibited release of HMGB-1 from the nucleus. *In vivo,* ASP-Lip@GelMA can effectively inhibit inflammation of local tissue after disc surgery and fill local tissue defects. This composite hydrogel system is a promising way to treat the recurrence of IDD after surgery without persistent complications.

## 1. Introduction

Low back pain (LBP) is not a fatal condition, but it constitutes a significant global public health problem [1,2]. One study indicated that intervertebral disc degeneration (IDD) is the most common reason for LBP [3]. Current therapies for LBP focus on surgery, which can significantly release nerve compression and attenuate pain caused by the protrusion of the nucleus pulposus (NP) [4]. The trauma of tissue caused by the operation will induce inflammation of local tissue, and serious inflammation will lead to the degeneration, and induce disease recurrence or the occurrence of other diseases [5]. Therefore, it is very necessary to inhibit postoperative inflammation.

Inflammation is an important and complex pathophysiological process. Tumor necrosis factor-α (TNF-α) can upregulate metalloproteinase activity and gene expression, reducing the synthesis of collagen and proteoglycans. Additionally, interleukin (IL)-6 could induce aggregation and activation of immune cells and release inflammatory mediators [6,7]. Recent studies have examined the inflammatory microenvironment. The inflammatory microenvironment mainly refers to inflammatory cells and inflammatory factors, which become essential pathological factors in the occurrence and development of inflammatory diseases. Additionally, under the influence of the inflammatory microenvironment, the reaction time of inflammation differs [8,9]. For example, after discectomy, the inflammatory cycle can be

Peer review under responsibility of KeAi Communications Co., Ltd.
* Corresponding author.
** Corresponding author.
*** Corresponding author: Department of Orthopaedics, The First Affiliated Hospital of Soochow University, Suzhou, Jiangsu, 215006, PR China.
*E-mail addresses:* maohq@suda.edu.cn (H. Mao), lyl1987@nsmc.edu.cn (Y. Li), szgengdc@163.com (D. Geng).
[1] Contributed equally to this work.

https://doi.org/10.1016/j.bioactmat.2020.07.008
Received 6 April 2020; Received in revised form 3 July 2020; Accepted 17 July 2020

sustained for more than 14 days [7,10]. Furthermore, studies have shown that TNF-α, IL-1β and IL-6 play an important role in the acute phase [7]. The regulator high mobility group box 1 (HMGB1) determines the cycle of chronic inflammation [11,12]. Therefore, controlling the expression of inflammatory factors is very important for the control of postoperative inflammation after discectomy.

Currently, the control of postoperative inflammation mainly depends on oral drugs, such as celecoxib. However, due to the lack of vascular tissue in the intervertebral disc, oral medication alone cannot provide effective concentrations locally, and for some patients, such as those with gastric ulcers and hypertension, there are unavoidable additional side effects [13]. Controllable release of aspirin could decrease potentially side effects and allowed less administration [14]. Other methods, such as physical therapy strengthening and muscle training, are also considered to improve clinical symptoms after surgery, but there is no effective research and clinical effect statistics [4,15]. Therefore, injecting anti-inflammatory functional materials into the defect tissue after discectomy is a feasible strategy to control the inflammation microenvironment locally.

Gelatin modified by methacrylic anhydride (GelMA) hydrogel offers a novel choice as a carrier for controllable release of anti-inflammatory drugs due to its similarity to the natural extracellular matrix and excellent biocompatibility [16,17]. In addition, a photocrosslinking agent to GelMA can be used for local curing and is beneficial for the repair of tissue defects. Liposomes in the hydrogel delivery system could increase the release of hydrophobic drugs and further improve bioavailability, avoid burst drug release, and reduce toxicity and side effects. Meanwhile, GelMA could protect the integrity of liposomes and improve their stability [18,19]. In this study, we designed a photocrosslinkable GelMA hydrogel-based drug delivery system with improved aspirin release, injectability and fixation properties to prevent tissue re-protrusion and degeneration after discectomy. After injection, the composite GelMA drug delivery system could fill the defect and provide the necessary mechanical support after being crosslinked, alleviating the degeneration process aggravated by mechanical changes. The locally released aspirin could inhibit the postoperative inflammatory response of residual tissue and effectively delay the development of degeneration. Finally, aspirin and GelMA have been widely applied and intensively studied, and their safety and reliability have been widely verified, thus supporting the clinical application of the GelMA drug delivery system (see Scheme 1).

## 2. Methods and materials

### 2.1. Ethics statement

This study was approved by the First Affiliated Hospital of Soochow University Ethics Committee (No. 201903A012). Animal operations, interventions, treatments, and feed were provided in accordance with the guidelines of the animal center of Soochow University, Suzhou, China.

### 2.2. Reagents and antibodies

Aspirin (ASP), methacrylic anhydride (CAS: 760-93-0) and PI (CAS: 106797-53-9) were purchased from Sigma-Aldrich (St. Louis, USA). Additionally, rabbit anti-rat collagen-2 (COL-2) (ab34712), matrix metalloproteinase-3 (MMP-3) (ab52915), IL-1β (ab9722), TNF-α (ab6671), IL-6 (ab9324) and goat anti-rabbit immunoglobulin G H&L (Alexa Fluor® 488) (ab150077) antibodies were purchased from Abcam (Shanghai, China). β-Actin and DAPI were purchased from Beyotime (Shanghai, China). Lecithin (CAS: 8002-43-5) and cholesterol (CAS: 57-88-5) were purchased from Macklin (Shanghai, China). Gelatin (lot No. 180LB8) was purchased from Rousselot (Angoulême, France).

### 2.3. Fabrication and characterization of liposomes

ASP-loaded liposomes (ASP-Lips) were fabricated by the film dispersion method, according to previous reports [16,20]. Lipids and ASP were dissolved in chloroform concurrently (50:1, w/w). The solution of these composite materials was to remove the organic solution at a speed of 100 r/min in the rotary vacuum evaporator, and the temperature of the water bath was 30 °C. After gentle evaporation, a homogeneous thin foveolate film formed in the flask. Furthermore, preheated deionized water (DI water) was utilized to hydrate the film with rotation (100 r/min) and heating (30 °C). Subsequently, primary drug-loaded liposomes were generated, and the solution was ultrasonicated and extruded through polycarbonate membranes with different diameters (0.45 μm and 0.22 μm). Then, ASP-loaded liposomes were fabricated. Under the protection of trehalose, these liposomes were lyophilized to produce powdered ASP-Lips.

ZetaSizer (Zen 4003, Malvern Instruments, Ltd, UK) was used to evaluate the properties of the ASP-Lips (the average particle size, zeta potential, and size distribution). In addition, transmission electron

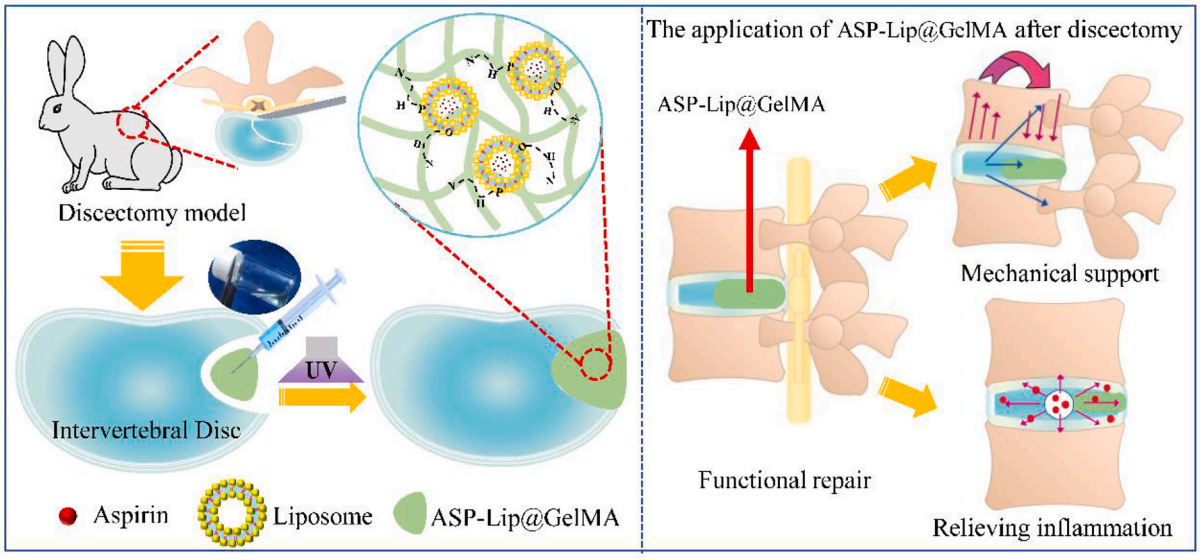


**Scheme 1.** Composite hydrogel (ASP-Lip@GelMA) for preventing recurrence after partial discectomy.

microscopy (TEM) (FEI Tecnai G-20) was used to observe the ASP-Lips morphology.

Centrifugal ultrafiltration was used to separate unloaded ASP, and the concentration of the free drug was measured via high-performance liquid chromatography (HPLC) to evaluate the ASP entrapment efficiency. After centrifugation, the sedimented solution was gathered and examined to evaluate the concentration of the unloaded drug by HPLC using the ODS column analysis at room temperature. For ASP, the mobile phase included methyl cyanide and water (250:750 v/v). The flow rate was set to 1.0 mL/min, with a 207-nm detection wavelength. To further observe the drug release behavior of ASP-Lips, the sample was immersed in 50 mL of fresh PBS. Then, at fixed time intervals, the midum was colloected, and HPLC was used to evaluate the concentration of ASP.

### 2.4. Hydrogel preparation and investigation

#### 2.4.1. The preparation of gelatin-methacryloyl

GelMA was prepared under the previously reported procedure [21]. Twenty grams of gelatin was added to PBS (200 mL) at 60 °C under constant stirring until the gelatin was completely dissolved. Next, 16 mL of methacrylic anhydride was added dropwise to the gelatin within 1 h. After 2 h, 800 mL of preheated PBS was added dropwise within 15 min, followed by continuous stirring to stop the reaction. Afterward, products were sealed in a dialysis bag (MW = 8000–12000) and dialyzed for a week to remove unreacted methacrylic anhydride. After 7 days, the solution was collected from the dialysis bag and heated to 60 °C, and the solution was then filtered through a microporous membrane (220 nm). Finally, the fluid was stored at −80 °C for 12 h and lyophilized to produce GelMA.

#### 2.4.2. Hydrogel preparation

A total of 60 mg of lyophilized ASP-Lips powder was weighed and dissolved in 1 mL of DI water. The precrosslink solution (ASP-Lip@GelMA) was prepared from PI (w/w) and GelMA (20%, w/w). At the same time, 60 mg of the same quality ASP as that contained in the ASP-Lip@GelMA was weighed and dissolved in 1 mL of DI water to prepare the ASP-GelMA precrosslink solution. Then, these solutions were poured into a module. Ultraviolet (UV) lighting at 6.9 $mW/cm^2$ was utilized to crosslink the two solutions; for each hydrogel, the lighting process lasted 10 s.

#### 2.4.3. Hydrogel characterization

After freeze-drying, the ASP-Lip@GelMA sample was fixed on the specimen platform. Gold produced by the sputter coater was used to cover the sample, and the samples were observed by SEM. Randomly selected parts of the hydrogel were selected for further analyses of the interaction between the liposomes and the hydrogel.

The mechanical properties of the ASP-GelMA (control group) and ASP-Lip@GelMA were observed by an equivalence force test instrument in compression tests. To evaluate the swelling ability of the hydrogel, the samples were first freeze-dried. Then, the hydrogels were weighed, and this weight was regarded as the original weight ($W_0$). Afterward, the hydrogels were immersed in PBS. At varying time points, the hydrogels were weighed, and the amount was recorded as $W_t$. Then, the swelling percentage of the hydrogel was calculated according to the following formula:

$$Swelling\ \ percentage\ \ (\%) = \frac{W_t - W_0}{W_0} \times 100\%$$

Moreover, the degradation of hydrogels was also examined in this study. Hydrogels were soaked in PBS at 37 °C for 1 day to achieve the equilibrium swelling state. Then, the original mass ($W_0'$) was recorded. The degradation test was performed in collagenase-2 solution (2 U/mL) at 37 °C. At set time points, the remaining masses were regularly recorded as $W_t'$, and degradation kinetics were tracked using the degradation formula:

$$\text{Remaining masses } (\%) = \frac{W'_t}{W'_0} \times 100\%$$

The release behavior of ASP was measured in the ASP-GelMA and ASP-Lip@GelMA groups *in vitro*. Specifically, ASP-GelMA hydrogel and ASP-Lip@GelMA hydrogel were soaked in the PBS for varying times. Each time, all medium was completely replaced with the fresh PBS. Then, the concentration of ASP in these medium was detected by HPLC-UV.

### 2.5. Nucleus pulposus cell (NPC) culture

Nucleus pulpous cells were collected from caudal discs 1 to 5 [22]. The nucleus pulposus tissues were digested with collagenase-II (0.5%) for 2 h at 37 °C. Then, the digested tissues were cultured with the F-12 DMEM (Gibco, USA) with 10% fetal bovine serum (Gibco, USA) and 1% antibiotics (Gibco, USA). Incubator parameters were set at 37 °C and 5% carbon dioxide. When cells reached confluence, harvesting was completed using Trypsin- EDTA (0.25%) (Gibco, USA). The NPCs were divided into three experimental groups, as follows: (1) Control: the NPCs were cultured on the GelMA-liposomes (GelMA-Lip) without ASP for 24 h; (2) Vehicle: the NPCs were cultured on the GelMA-Lip without ASP, and the lipopolysaccharides (LPS) (1 μg/mL) was added for 24 h; (3) ASP-Lip@GelMA group: the NPCs were cultured on the ASP-Lip@-GelMA, and the LPS (1 μg/mL) was added for 24 h.

### 2.6. Cell adhesion and viability assay

NPCs ($5 \times 10^4$ cells/well) were cocultured with different material groups in 48-well plates. Then, the morphology of the NPCs was observed through SEM. NPC viability were measured with the CCK-8 kit (Dojingdo, Japan), and a live-death assay kit (Sigma-Aldrich, USA) was used to observe the influence of the material on NPCs.

### 2.7. Enzyme-linked immunosorbent assay (ELISA)

IL-6, TNF-α, and HMGB1 concentrations in the cell culture supernatants were measured by the ELISA kit (Shino-Test, Japan; R&D, USA). Briefly, NPCs were pretreated with/without aspirin and incubated with IL-1β (10 ng/mL). Then, culture supernatants were collected and transferred to anti-IL-6-, TNF-α- or HMGB1-coated wells. Secondary polyclonal antibody was added for 2 h, followed by the addition of substrate solution to the reaction for 15 min. Finally, the absorbance (450 nm) was measured using the microplate reader.

### 2.8. Real-time polymerase chain reaction (RT-PCR)

RNA was extracted from NPCs using TRIzol reagent (Invitrogen, USA). Each reaction volume of PCR amplification was 20 μL, as follows: 1 μL of complementary DNA, 10 μL of Master Mix (Hayward, US), 0.5 μL of each primer and 8 μL of DEPC water. The sequence of primers is shown in Table 1.

### 2.9. Western blot assay

Total protein was isolated using RIPA buffer (Beyotime, China). Then, 30 μg of protein was separated by SDS-PAGE and transferred to a polyvinylidene difluoride membrane (Bio-Rad, USA). Following blocking with BSA (5%), the membrane was incubated with the different primary antibodies and β-actin (1:5000) overnight at 4 °C. Then, the samples were washed for 20 min with TBST, followed by secondary antibodies. Last, the bands were added to the electrochemiluminescence reagent (ThermoFisher, USA), and the intensity of the sample bands was quantified with Image Lab 3.0 software (Bio-Rad, USA).

**Table 1**
The primer sequence of RT-PCR.

| Gene name | NCBI ID | Forward primer (5′-3′) | Forward primer (5′-3′) |
|---|---|---|---|
| GAPDH | 24383 | GCAAGTTCAACGGCACAG | CGCCAGTAGACTCCACGAC |
| Collagen 2 | 25412 | GAGTGGAAGAGCGGAGACTACTG | CTCCATGTTGCAGAAGACTTTCA |
| Aggrecan | 58968 | TACGACGCCATCTGCTACAC | TCGAAGATGGGCTTTGCAGT |
| MMP-3 | 171045 | TTTGGCCGTCTCTTCCATCC | GCATCGATCTTCTGGACGGT |
| MMP-13 | 171052 | TCCATCCCGAGACCTCATGT | AGCATCATCATAACTCCACACG |
| ADAMTS-4 | 66015 | CGTTCCGCTCCTGTAACACT | TTGAAGAGGTCGGTTCGGTG |
| ADAMTS-5 | 304135 | GCCTGCAAGGGAAATGTGTG | GGCGGAAAGATTTGCCGTTAG |

### 2.10. Immunocytochemical (ICC) staining

NPCs were cultured in 48-well culture slides and fixed in formaldehyde (4 °C) for 10 min. Then, samples were incubated with 5% FBS for 1 h. Next, NPCs were incubated with primary antibodies of COL-2 (1:500) or MMP-3 (1:500) for 16 h. The next day, the NPCs were incubated with the Alexa Fluor 488 (1:1000) secondary antibody for 2 h. Then, the samples were counterstained with DAPI for 20 min.

### 2.11. Experimental animals

Male Sprague-Dawley (SD) rats (3 months -old, 450 ± 50 g) and male New Zealand white rabbits (1 year -old, 4000 ± 500 g body weight) were purchased from the Experimental Animal Center of Soochow University (Suzhou China).

### 2.12. Surgical procedures and groups

In this study, four groups were established, which included a normal group (control group), a defect group (vehicle group), an ASP-GelMA treatment group, and an ASP-Lip@GelMA treatment group. All animals were fasted for 12 h and deprived of water for 6 h before anesthetizing them with an intramuscular injection of 2% pentobarbital. The fur of the animals was removed from the dorsal surface. Through the anterolateral approach, we contacted the front of the spine. The IDD model was established by rabbits via disc puncture with an 18G needle at lumbar vertebrae 2–3, 3–4 and 4–5; the defect of the annulus fibrosus was considered established after extirpation of the intervertebral disc [23,24]. After puncturing the annulus fibrosus, the procedures used in previous studies were followed to ensure the defect was established [25–27]. To exclude the effects of individual differences in laboratory animals, we performed the four operations on the same rabbit. We defined the L1-2 rabbits as the control group (normal disc), L2-3 as the vehicle group (degeneration disc), L3-4 as the ASP-Lip@GelMA injection group and L4-5 as the ASP-GelMA injection group. To exclude the influence of the operation, the injected volume was 4 μL, the depth was 5 mm, and the position was the nucleus pulposus center. All injections were performed with a 1 mL injector through an 18G needle, and this did not induce degenerative disc changes.

### 2.13. In vivo mechanical compression test

Rabbits were selected randomly, overdosed with anesthesia, and executed with pentobarbital sodium. To avoid errors in the mechanical test caused by differences in the anatomical structure, we chose the L2-3 vertebral body as the experimental object. The tooth powder (Boer Chemical, Shanghai) was embedded in the upper and lower ends of the vertebral bodies. Then, they were polished to keep them parallel. Each group (n = 5) was tested in the mechanical testing machine (Hengyi, Shanghai).

### 2.14. Imaging examination and analysis

After 1 and 2 weeks following initial annulus puncture, 20 rabbits were randomly selected for X-ray and MRI assessments. Lumbar computed radiography (CR) imaging was performed by a Small Animal Digital X-ray Imaging System (SEDECAL, Spain), and MRI tests were performed via a 3.0 T system (Siemens, German).

The radiographic results were analyzed by a PACS system (Neusoft, China) by two independent radiologists. We obtained the value of the disc height index (DHI) according to Lu [28]. The change in DHI was expressed as DHI %. Referring to the modified Thompson classification [29], the T2-weighted MRI images were classified as grade I to grade IV [27].

### 2.15. Histological and immunohistochemical (IHC) analyses

Excessive pentobarbital sodium anesthesia was used to euthanize the rabbits. Samples were fixed in formalin (10%) for 3 days and decalcified through EDTA (10%) for 40 days. After embedded into the wax, samples were stained with H&E and safranin O - Fast green. Histological grading was performed as described by Masuda [29]. The expression of TNF-α (1:200), IL-1β (1:1000), IL-6 (1:1000), collagen-2 (1:200), and MMP-3 (1:100) in the intervertebral disc tissues was assessed by IHC staining.

### 2.16. Statistical analysis

In this study, data are expressed as the mean ± standard deviation (SD) or fold change. All of the experiments were conducted at least three times independently. Statistical significance was determined using one-way analysis of variance (ANOVA) with Tukey's post hoc multiple comparisons tests. $^{*}P < 0.05$ was considered statistically significant.

## 3. Results

### 3.1. Composite hydrogel characterization

As the fundamental element of the composite hydrogel system, ASP-Lips were comprehensively investigated (Fig. 1A–D). As shown in Fig. 1A and B, the diameter and zeta potential of ASP-Lips were explored by dynamic light scattering (DLS) and electrophoretic light scattering (ELS). The results indicated that the median diameter of ASP-Lips was approximately 141.8 nm, and the median zeta potential was 11.2 mV. Furthermore, the morphology of ASP-Lips was explored by transmission electron microscopy (TEM), as shown in Fig. 1C. The ASP-Lips exhibited a round appearance and bilayer structure. The liposome loaded with ASP significantly improved the hydrophobicity of the ASP. Within 24 h, the aspirin release was close to 80%, which could improve the local bioavailability of the drug (Fig. 1D). The interaction between ASP-Lips and the GelMA hydrogel network is shown in the schematic diagram in Fig. 1E. The hydrogel exhibited excellent morphological properties (rounded and uniform-sized pores and a thin wall) as observed by scanning electron microscopy (Fig. 1F). Then, a random area with some spherical particles on the surface of the hydrogel was selected, and the diameters of the particles were evaluated. A diameter of 126.3 nm was observed, similar to the diameter of the ASP-Lips

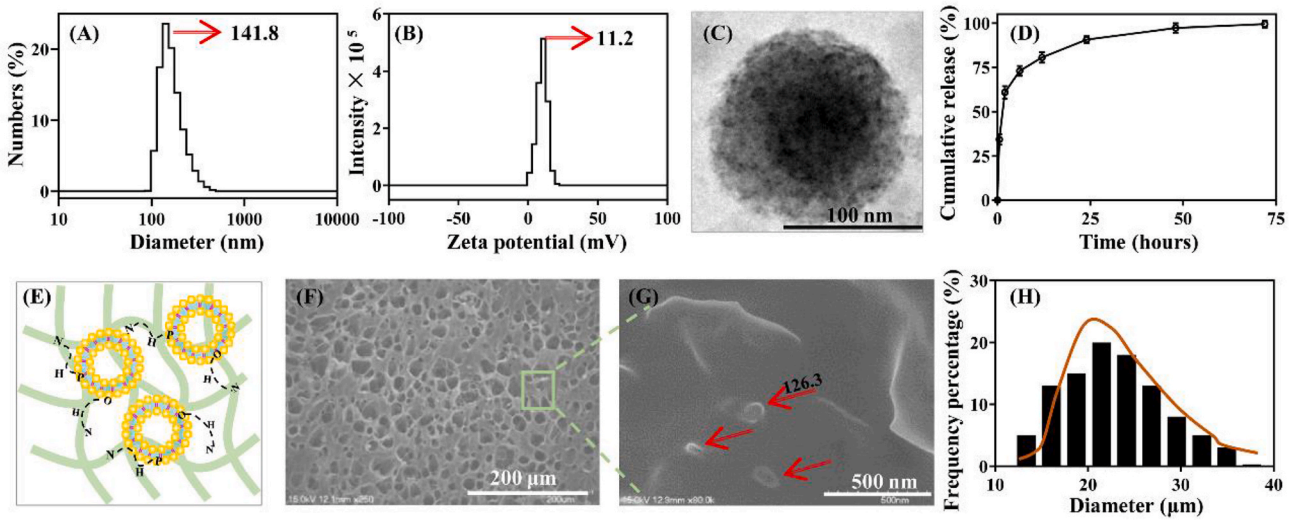


**Fig. 1.** Characterization of the hydrogels and ASP-Lips. (A) The ASP-Lips particle size. **(B)** The zeta potential of ASP-Lips. **(C)** TEM images of ASP-Lips; scale bar, 100 nm. **(D)**The release percentage of ASP-Lips. **(E)** Schematic diagram of the interaction between ASP-Lips and the GelMA hydrogel. **(F)** SEM images of the hydrogel; scale bar, 200 μm. **(G)** The magnification of the selected area; scale bar, 500 nm. **(H)**The pore size distribution.

(Fig. 1G). Next, 100 pores were randomly selected, and the average diameter was 21.45 ± 10.76 μm (Fig. 1H).

The process of crosslinking is shown in Fig. 2A and B. After 10 s of UV irradiation, the pre-crosslinking solution formed the composite hydrogel. As shown in Fig. 2C and D, the micro-crosslinking of the liposomes and hydrogel limited the process of water penetration and decreased the rate of composite material degradation. The swelling ratio of the aspirin-loaded liposomes@gelatin-methacryloyl (ASP-Lip@GelMA) ranged from 371.81 ± 2.48% to 384.92 ± 6.64% and was always lower than that of the aspirin-gelatin-methacryloyl (ASP-GelMA), which ranged from 538.53 ± 19.43% to 617.93 ± 78.55% during the 24 to 100-h period (Fig. 2C)($P < 0.05$). Similarly, at day 16, the mass of the remaining ASP-GelMA was 0 g. However, the ASP-Lip@GelMA was completely degraded until day 24 and was longer than the ASP-GelMA at 37 °C (Fig. 2D). Controlled ASP release was investigated in ASP-Lip@GelMA and ASP-GelMA. As shown in Fig. 2E, ASP-Lip@GelMA (85.43 ± 2.30%) exhibited a higher cumulative release percentage than ASP-GelMA (68.89 ± 1.14%) ($P < 0.05$), which is mainly attributable to the improvement in the dispersion of ASP in the ASP-GelMA by the liposomes. In the hydrogel network, nitrogen is likely to form the hydrogen bond on the surface of the liposomes through phosphorus and oxygen, which will enhance the mechanical strength in the composite hydrogel (Fig. 2F–I).

### 3.2. Cell adhesion and proliferation on the hydrogel

To determine the biological safety of composite hydrogel, we investigated the proliferation of NPCs in different material groups. The results showed that the hydrogel and drug combination did not influence NPC proliferation; moreover, the proliferation in the ASP-Lip@GelMA group was greater than that in the other groups at 1–7 days (Fig. 3A). NPCs were seeded in the different material groups to examine the proliferation capacity. The co-culture results are shown in Fig. 3B. After 1 day, the two material surfaces showed the same level of NPC adhesion. Additionally, there was no significant difference in the materials group compared with the control group. NPC pseudopodia were widely connected with materials and cells, as well as between cells themselves, covering all material surfaces and becoming confluent.

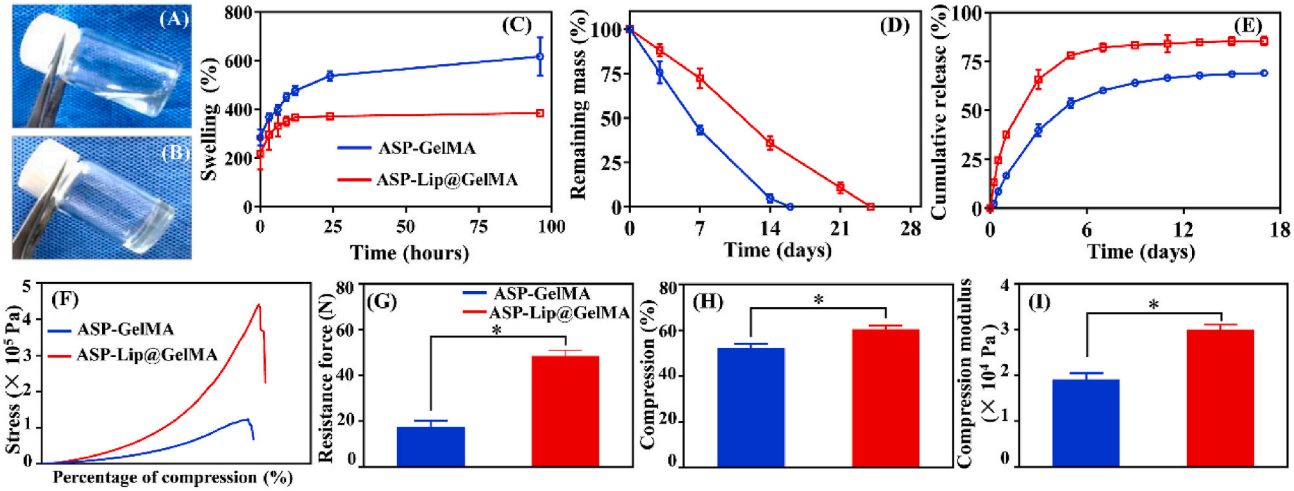


**Fig. 2.** Characterization and mechanical examination of the hydrogels. (A) ASP-Lip@GelMA solution. **(B)** The ASP-Lip@GelMA after photocrosslinking. **(C)** Mass Swelling curve of ASP-Lip@GelMA and ASP-GelMA. **(D)** Remaining mass percentage of ASP-Lip@GelMA and ASP-GelMA. **(E)** The drug release profile of ASP-Lip@GelMA and ASP-GelMA. **(F)** ASP-Lip@GelMA and ASP-GelMA compression experiments. **(G)** Resistance force. **(H)** Percentage of compression. **(I)** Compression modulus. (*$P < 0.05$ vs. ASP-GelMA group).

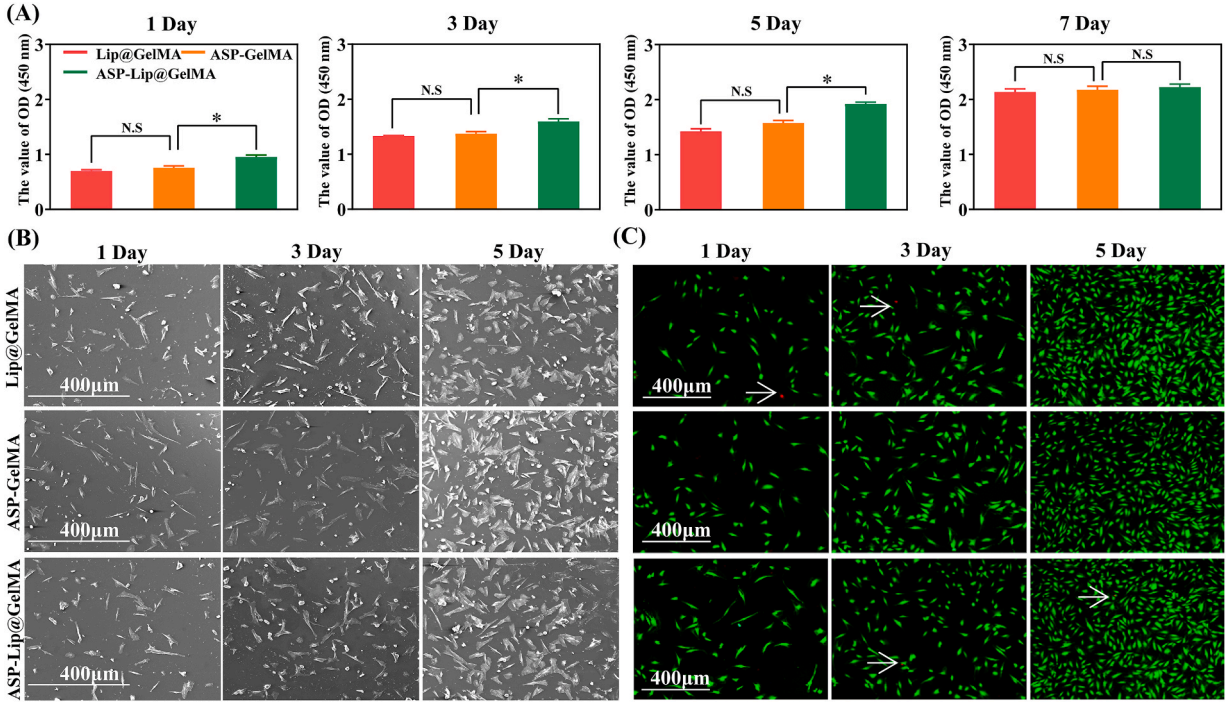


**Fig. 3.** Cell adhesion and proliferation of NPCs in the hydrogel. (A) The proliferation of NPCs were cultured on different materials for 1, 3, 5, and 7 days was assessed using a CCK-8 kit. **(B)** SEM images of cells on the hydrogel after seeding for 1, 3, and 5 days; scale bar, 400 μm. **(C)** Live−dead staining of cells cultured on the hydrogel for 1, 3, and 5 days. White arrow: dead cell. Green: living cell. Red: dead cell; scale bar, 400 μm (*$P < 0.05$ vs. ASP-GelMA group; no significant difference is indicated with N.S.).

Furthermore, we tested the toxicity of the materials via live-dead staining (Fig. 3C). The data showed that there was no effect on cell activity among the different material groups after 5 days.

### 3.3. Evaluation of the in vitro anti-inflammatory effect of the composite hydrogel

To identify the anti-inflammatory effect of ASP-Lip@GelMA *in vitro*, we performed an ELISA on NPCs stimulated with IL-1β and cocultured with the test materials. Compared with the control group, the vehivle group (IL-1β-treated) exhibited increased expression levels of TNF-α (~32.91-fold) and interleukin-6 (IL-6) (~4.04-fold; $P < 0.05$). Additionally, the ASP-Lip@GelMA group showed effective anti-inflammatory effects (TNF-α: ~0.22-fold; IL-6: ~0.34-fold) ($P < 0.05$).

The RT-PCR results indicated that IL-1β treatment reduced the expression of COL-2 (~0.21-fold) and aggrecan (~0.19-fold) while increasing the expression of MMP-3 (~2.12-fold) and MMP-13 (~3.11-fold) ($P < 0.05$). Furthermore, compared with the control group, the IL-1β-treated group displayed noticeably increased expression of the ADAMTS-4 (~1.89-fold) and ADAMTS-5 (~2.33-fold) ($P < 0.05$). Importantly, the process of degeneration was reversed in the ASP-Lip@GelMA group (Fig. 4D–I). The same results were observed with ICC staining. Fig. 4J shows that the loss of collagen-2 was significantly prevented in the ASP-Lip@GelMA group; furthermore collagen-2 distribution around the nucleus was increased in NPCs, while the expression of MMP-3 was significantly inhibited. Additionally, in the ASP-Lip@GelMA group, ASP, which was released into the culture medium, alleviated the progression of degeneration by inhibiting the expression of proinflammatory factors.

It is worth noting that the HMGB1 expression was significantly increased (~9.31-fold) in the IL-1β-treated group ($P < 0.05$). The ASP-Lip@GelMA group showed significantly reduced HMGB1 expression (~0.51-fold, $P < 0.05$; Fig. 4C). To clarify the localization of HMGB1, we separated the nuclear and cytoplasmic fractions. The results showed that the level of HMGB1 in the nucleus decreased (~0.78-fold) after IL-1β treatment, while the level in the cytoplasm increased significantly (~1.47-fold, $P < 0.05$; Fig. 5A–D). The same results were observed for ICC staining (Fig. 5E). The HMGB1 was concentrated in the nucleus in the control group. Additionally, after IL-1β stimulation, HMGB1 was secreted into the cytoplasm, and its expression in the nucleus decreased.

### 3.4. The composite hydrogel material attenuates degeneration after surgery

Exogenous ASP-Lip@GelMA was injected in the rabbit disc defect model by needle puncture. We selected the destruction of the internal structure (in the IDD model) or the protrusion of the nucleus pulposus from the defect as the endpoints of the study. The composite hydrogel showed excellent sealing properties of the defect. Similar to the *in vitro* results, at the same research endpoint, the composite hydrogel enhanced the mechanical stability of the intervertebral disc compared with the vehicle group (Fig. 6A–E).

At 7 days after the initial annulus puncture, the vehicle group had a weaker MRI signal than the control group. The grade was 3.60 ± 0.31, and the difference became more obvious at 14 days (4.00 ± 0.30; Fig. 7A and B). ASP-Lip@GelMA treatment efficiently increased the MRI signal intensity and decreased the degeneration grade compared with the vehicle treatment. Throughout the study cycle, the CR imaging showed that a normal DHI% was maintained in the ASP-Lip@GelMA group (from 89.17 ± 11.22% to 84.81 ± 21.52%) compared with the vehicle group (from 75.15 ± 7.92% to 71.17 ± 12.35%) ($P < 0.05$). However, the intervertebral height still gradually decreased as the degeneration progressed (Fig. 7C and D).

The H&E staining (Fig. 8A) showed a defect of the annulus fibrosus (AF) and a severe decrease in nucleus pulposus (NP) in the defect group. However, the defect was reduced in the ASP-Lip@GelMA treatment group. The histological grade was 6.33 ± 0.57 in the ASP-Lip@GelMA group and 14.33 ± 3.05 in the vehicle group ($P < 0.05$; Fig. 8C). In the ASP-GelMA treatment group, there was no significant defect in the AF, and the decrease in the NP was not significantly changed, but it was slightly worse than that in the ASP-Lip@GelMA treatment group.

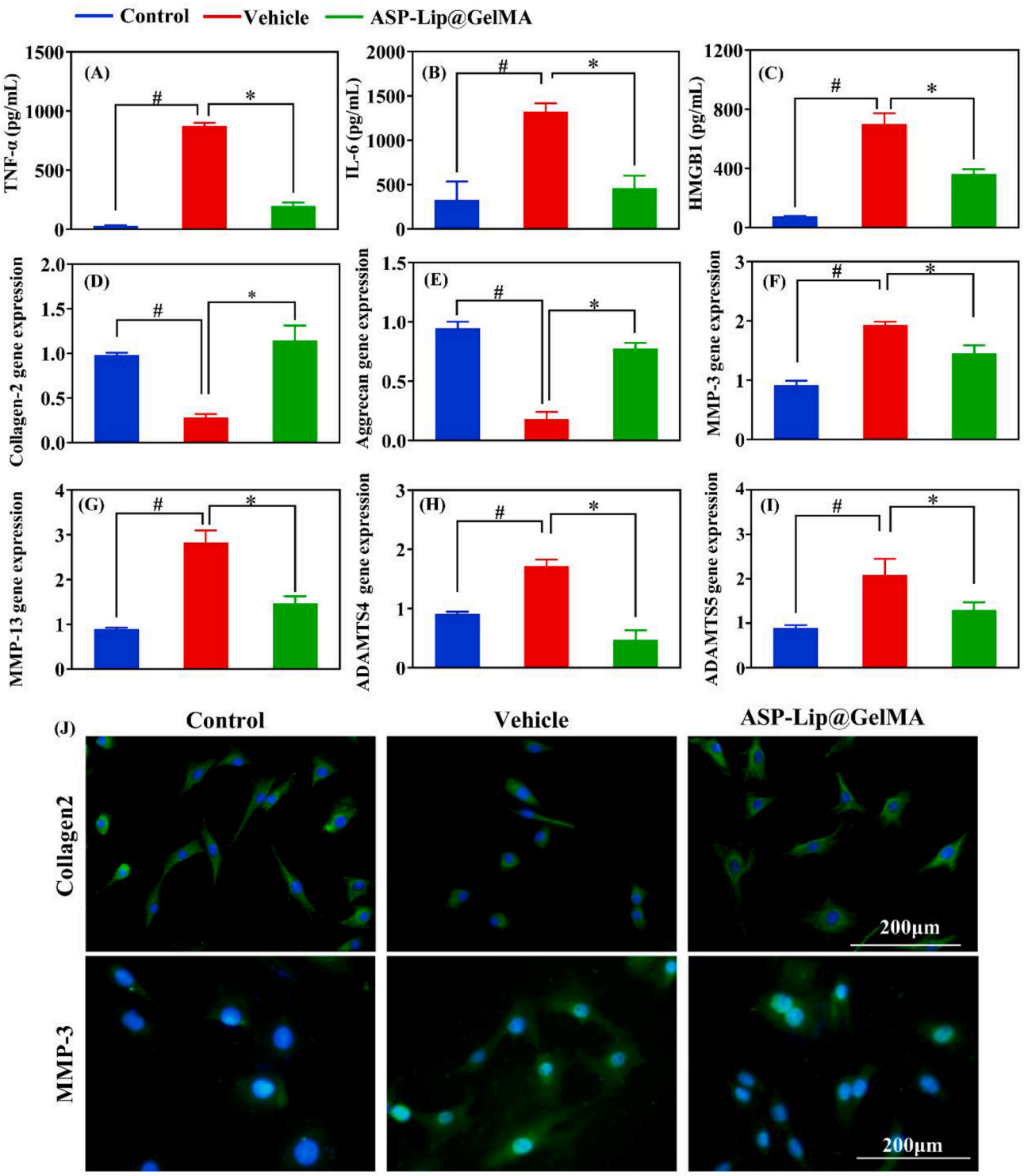


**Fig. 4.** ASP-Lip@GelMA attenuates inflammation and improves IDD. (A–C) The expression of TNF-α, IL-6 and HMGB1 was assessed. **(D–I)** RT-PCR results of collagen-2, aggrecan, MMP-3, MMP-13, ADAMTS-4, and ADAMTS-5 expression were obtained. **(J)** Representative image of immunofluorescence staining of collagen-2 and MMP-3 in NPCs; scale bar, 200 μm. (#$P < 0.05$ vs. control group, *$P < 0.05$ vs. vehicle group).

Safranin-O staining results are shown in Fig. 8B. In the control group, the NP was filled with collagen-2, while the vehicle group demonstrated reduced collagen-2 levels and a significant defect area in the nucleus pulposus. The structure within the ASP-Lip@GelMA and ASP-GelMA treatment groups was relatively intact, and the loss of collagen-2 was reduced. The histological grade (Fig. 8D) indicated that the ASP-GelMA (7.23 ± 1.02) and ASP-Lip@GelMA (7.02 ± 2.18) treatment groups had complete tissue, and the grading scores were much lower than those of the vehicle group (14.12 ± 2.08, $P < 0.05$).

Proinflammatory cytokines play essential roles in IDD. Therefore, we inspected the protective effects of ASP-Lip@GelMA in the rabbit IDD model. Results (Fig. 9AandB) showed higher MMP-3 (~7.47-fold), IL-1β (~2.34-fold), IL-6 (~2.30-fold) and TNF-α (~2.01-fold) expression in the vehicle group, while the ASP-Lip@GelMA group exhibited significantly downregulated expression of these cytokines ($P < 0.05$). Additionally, compared with the vehicle group, ASP-Lip@GelMA

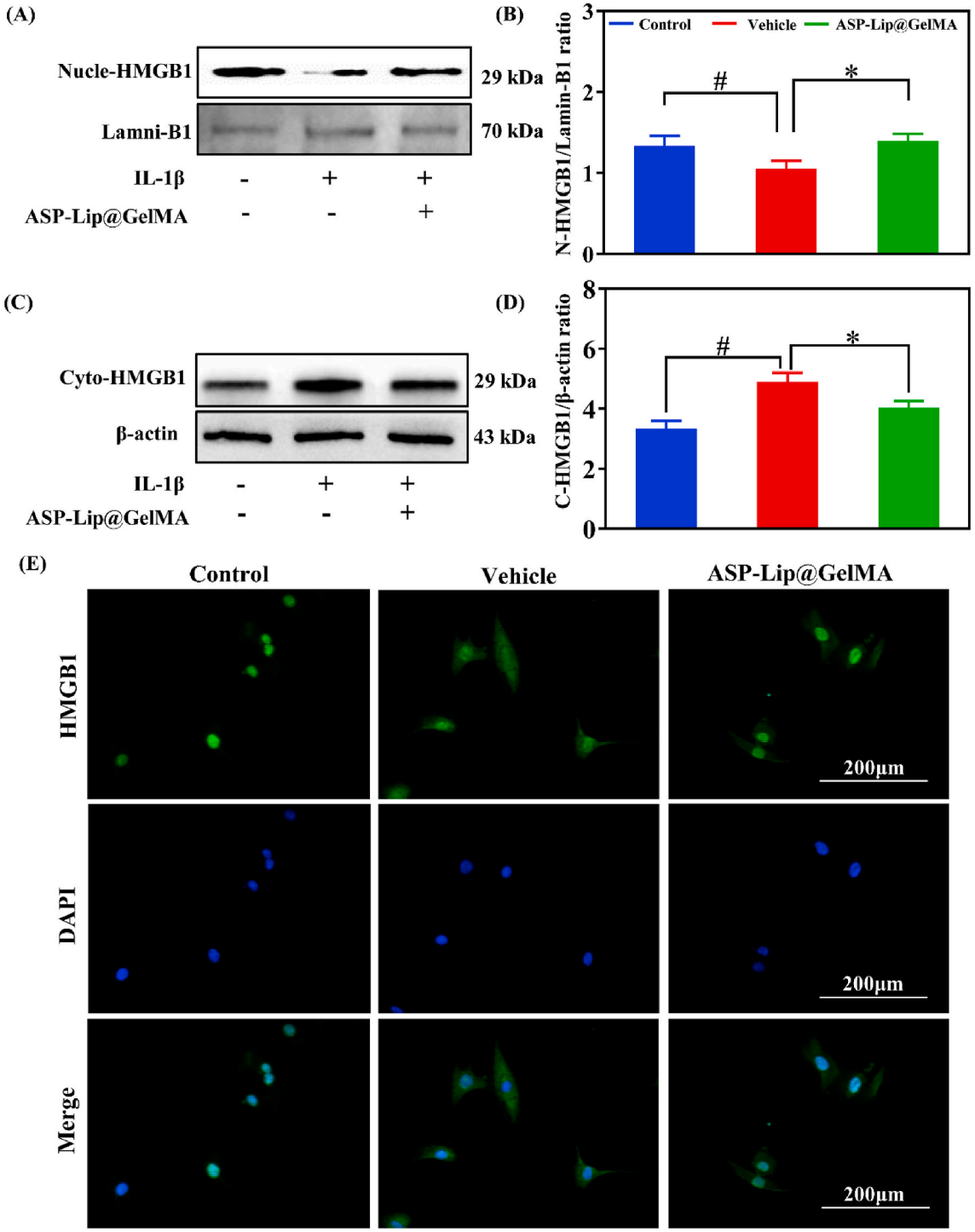


**Fig. 5.** ASP-Lip@GelMA attenuates HMGB1 expression in Cytoplasm. (A, B) WB results of nuclear HMGB1 and **(C, D)** cytoplasmic HMGB1 levels. **(E)** Representative image of HMGB1 immunofluorescence staining in NPCs; scale bar, 200 μm (*#P* < 0.05 vs. control group, **P* < 0.05 vs. vehicle group).

treatment obviously increased the expression of COL-2 (~3.08-fold, *P* < 0.05). These results indicated that the GelMA hydrogel drug delivery system can inhibit the inflammatory response and improve degeneration in *vivo*.

## 4. Discussion

One study shows that after lumbar discectomy, some changes of pathogeny, such as biomechanics change, will induce the recurrent lumbar disc herniation (RLDH) and reoperation [30]. Some researchers have reported that this incidence could reach 62% [31]. However, conservative treatment of RLDH remains unclear [30], and the re-operation cost is more than $30,000 [32]. Thus, the prevention of RLDH is an important subject in orthopedics research. This study demonstrated that the controllable release of aspirin from the GelMA hydrogel drug delivery systems attenuated inflammation and improved degeneration. The composite ASP-Lip@GelMA hydrogel sustained the mechanical stability of the local defect.

The most important source of reherniation is inflammation [33]. In inflammation, many inflammatory cells, such as neutrophils and

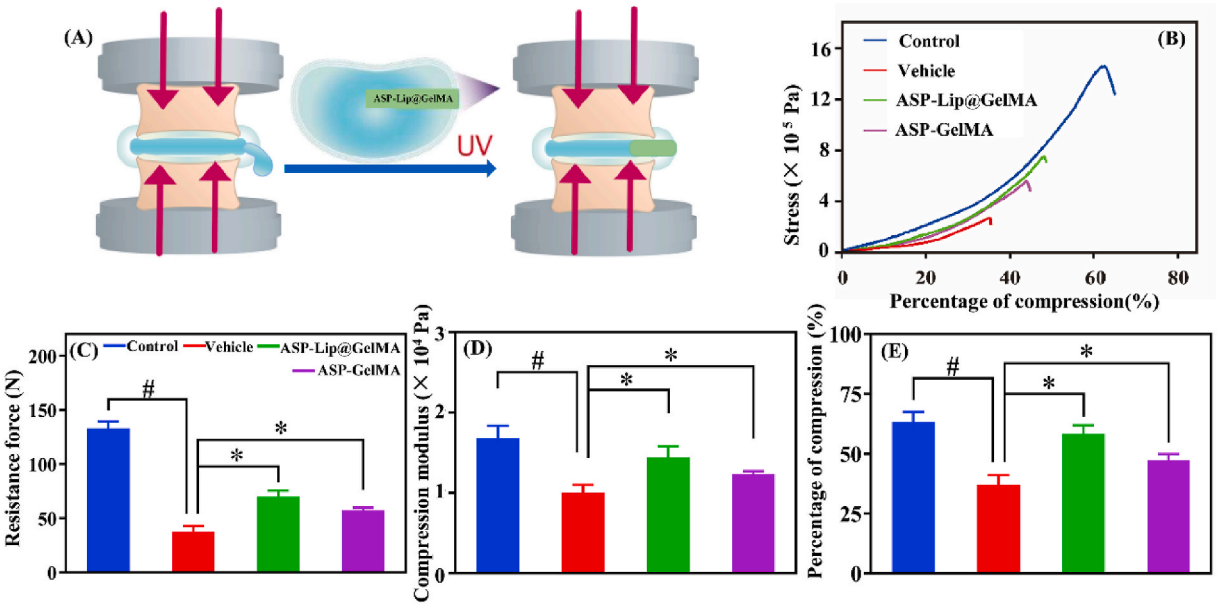


**Fig. 6.** *In vivo* compression test. (A) Compression test schematic diagram. **(B)** The compression results for the control, vehicle, ASP-Lip@GelMA, and ASP-GelMA groups. **(C)** The resistance force, **(D)** compression modulus, and **(E)** percentage of compression were assessed (#$P < 0.05$ vs. control group, *$P < 0.05$ vs. vehicle group).

lymphocytes, gather in the tissue to form an inflammatory response and have the functions of secreting corresponding molecular mediators of inflammation, such as IL-1β, IL-6, and TNF-α. Importantly, the increased concentration of inflammatory cytokines was observed in pathological disc tissue; additionally, with the increasing grade of degeneration, the concentration of these cytokines will increase [34,35]. These inflammatory mediators could affect the function of mitochondria and protein synthesis, leading to decreased extracellular matrix synthesis. Additionally, these inflammatory factors will upregulate the expression of MMPs and ADAMTSs, which will further

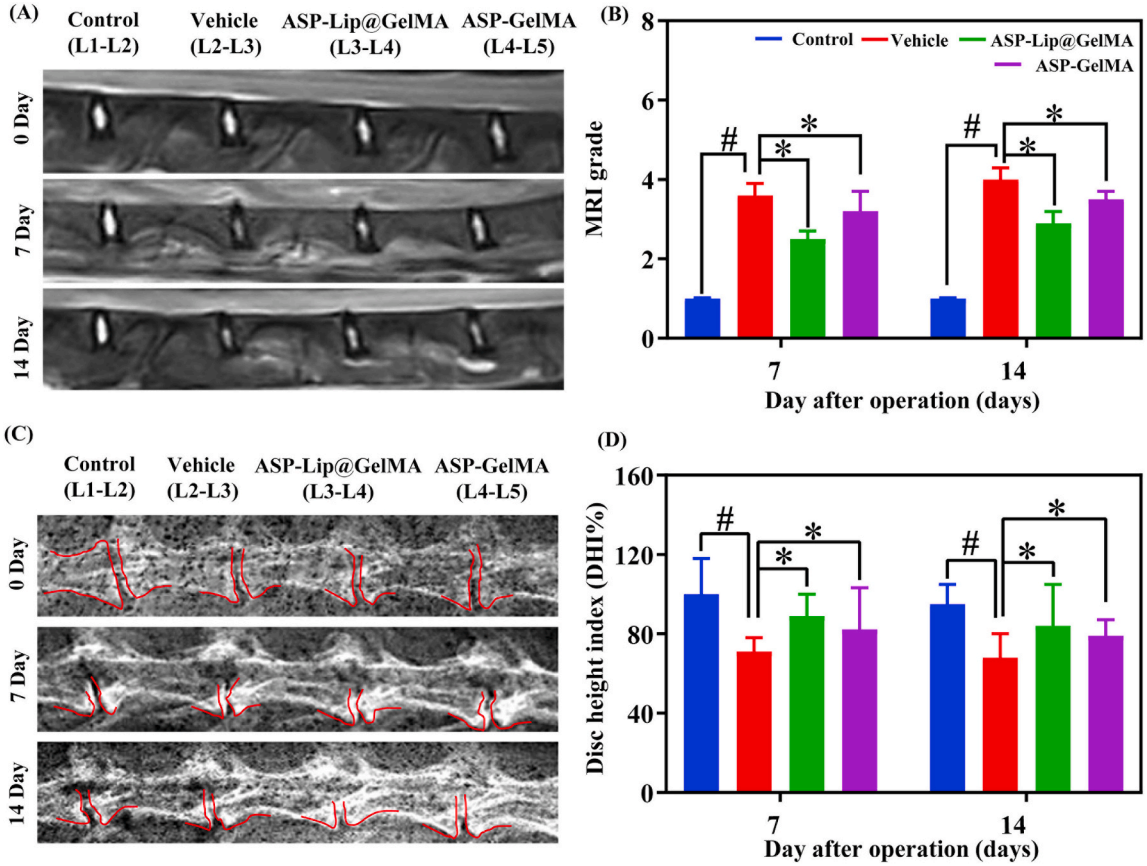


**Fig. 7.** Aspirin alleviates IDD *in vivo*. (A) Representative MRI showing the intervertebral disc signal intensity. **(B)** MRI grade statistics. **(C)** Representative X-ray image. **(D)** DHI %. (#$P < 0.05$ vs. control group, *$P < 0.05$ vs. vehicle group).

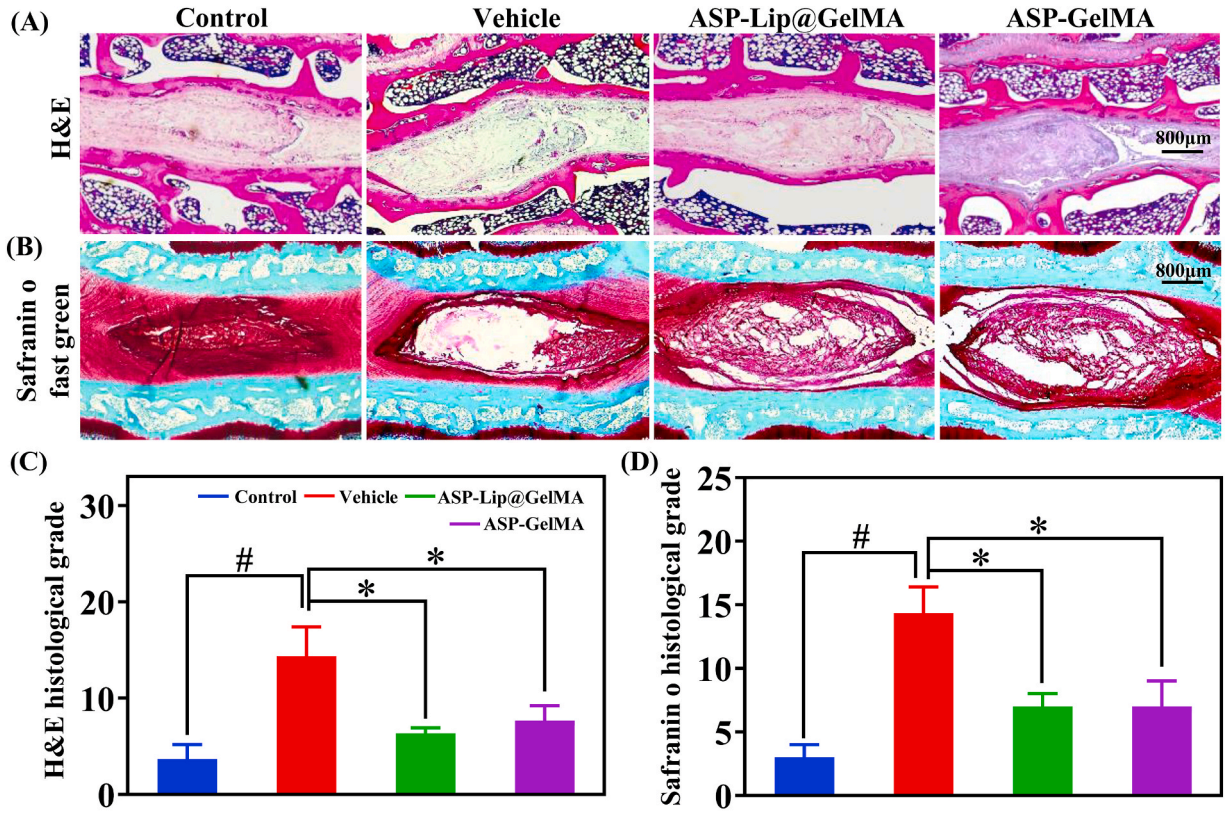


**Fig. 8.** Morphological staining *in vivo*. Representative paraffin sections with **(A)** H&E and **(B)** safranin-O staining. **(C, D)** Histological grades were determined (#$P < 0.05$ vs. control group, *$P < 0.05$ vs. vehicle group). Scar bar, 800 μm.

degrade collagen-2 and aggrecan. Furthermore, they will cause a decrease in the extracellular matrix and increased water loss, which will further cause spinal instability [33].

Recently, many studies have examined HMGB1, which can either act as a cytokine itself or function as a potent proinflammatory mediator [12,36,37]. Through active or passive release, HMGB1 could translocate from the nucleus to the cytoplasm and induce inflammation in the extracellular medium [38]. A positive correlation was found in the interaction between HMGB1 and inflammatory cytokines. The same phenomenon has been observed in IDD [36]. Anti-HMGB1 neutralization can attenuate LBP in rats [11]. Thus, there is strong evidence that HMGB1 could be a therapeutic target to attenuate the inflammatory reaction, leading to improved IDD. In the present study, the controlled release of aspirin affected HMGB1 expression and resulted in a decrease in inflammatory cytokine concentration. In our experiment, by inhibiting the migration of HMGB1 from the nucleus to the cytoplasm, we effectively controlled the inflammatory response, which provided a theoretical basis for regulating the inflammatory cycle.

Due to the important pathological role of inflammation in recurrence after discectomy, it is very important to control postoperative inflammation. However, the anatomical characteristics of the nucleus pulposus are not compatible with a single oral drug. Therefore, we designed and developed an injectable and anti-inflammatory hydrogel. GelMA is widely used in tissue engineering and various biomedical applications because GelMA closely resembles the native extracellular matrix of cells and has cell attachment and MMP-responsive peptide motifs. In this research, these advantages of GelMA allow nucleus pulposus cells to normally proliferate and have no adverse effects on cells [39,40]. Furthermore, GelMA can crosslink under the mild crosslinking conditions by a photoinitiator and form a 3D porous structure to carry both aspirin and ASP-Lips. Additionally, the properties, such as biodegradability and mechanical properties, of GelMA are tunable by adjusting the graft ratio of methacrylate. It can be easily combined with other hydrogels, such as alginate, chitosan, and composite PEG hydrogels for different biomedical applications [41,42]. As a self-assembling vesicle structure, the liposome can encapsulate both water-soluble and fat-soluble drugs. However, it is difficult to inject liposomes in localized intervertebral disc tissue because liposomes are in liquid form, which can easily leak from the injected area. In addition, it is difficult to maintain a specific local concentration. However, the porous structure of GelMA can provide space to contain and protect liposomes [18,19]. Additionally, the liposome could improve the dispersion of hydrophobic drugs in the GelMA hydrogel and improve the bioavailability of these hydrophobic drugs. At the same time, the slowed degradation of the ASP-Lip@GelMA further prolonged the drug release time. Importantly, GelMA and liposomes further form micro-crosslinked structures by hydrogen bonding. Our results showed that the ASP-Lip@GelMA exhibited excellent stress resistance to restore local mechanical stability compared with a single hydrogel.

In mechanical experiments, we used compression testing to observe the mechanical properties of hydrogels. Our results showed that ASP-Lip@GelMA could withstand more than 400 kPa pressure, which is close to some physiological conditions [43]. In addition, the spine is composed of the vertebral body and intervertebral disc, and previous studies have determined compressive modulus values ranging from 5 to 35 kPa [44–48]. In this study, the compression modulus of the ASP-Lip@GelMA system was approximately 15 kPa and suitable for injection into the nucleus pulposus. We will further study the application of mechanically enhanced hydrogels in the intervertebral disc and new drug carriers prepared by microfluidic technology in future studies [49].

## 5. Conclusion

In this study, we synthesized a crosslinked GelMA hydrogel (ASP-Lip@GelMA) with anti-inflammatory characteristics. We found that the

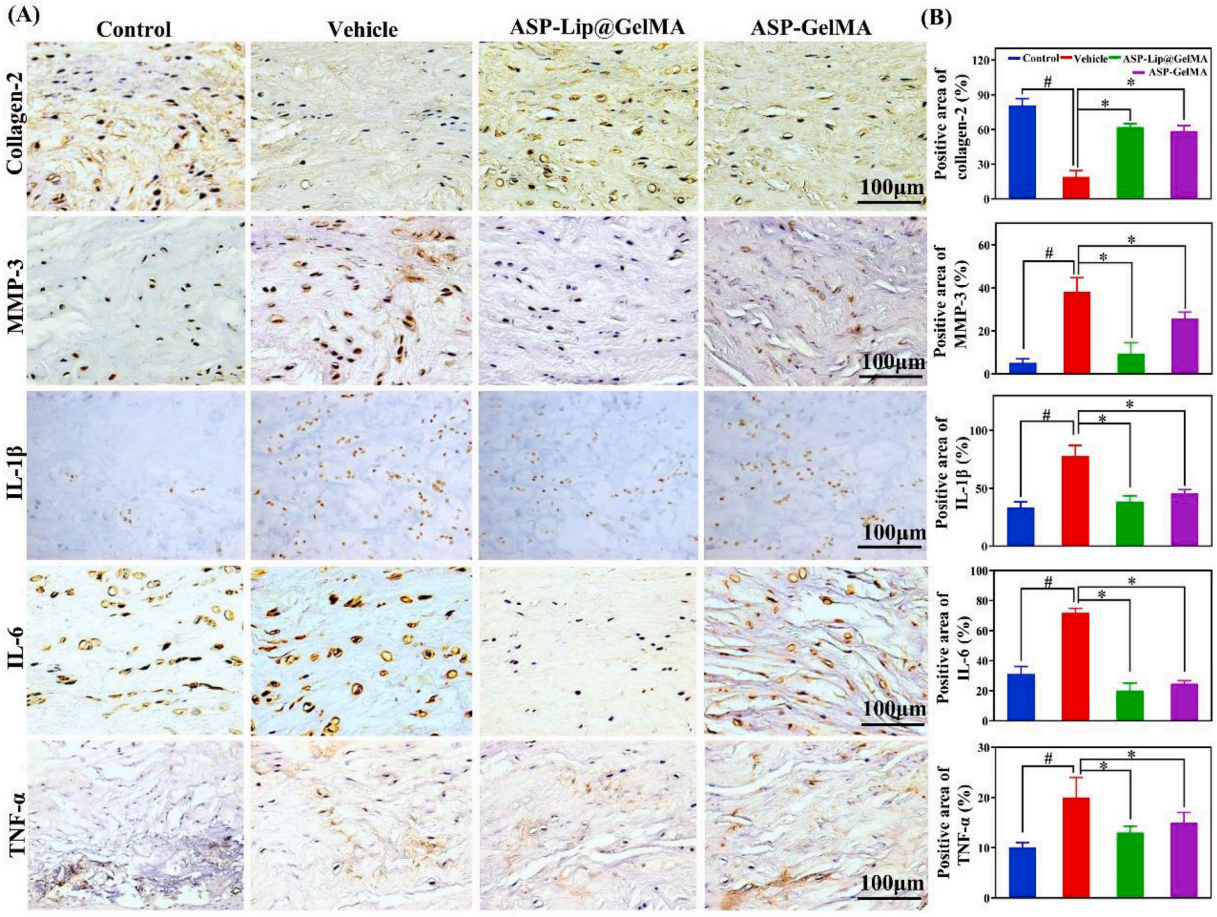


**Fig. 9.** IHC staining *in vivo*. (A) Representative paraffin-embedded section with IHC staining for collagen-2, MMP-3, IL-1β, IL-6 and TNF-α in nucleus pulposus tissue; scale bar, 100 μm. **(B)** Quantitative statistics for collagen-2, MMP-3, IL-1β, IL-6 and TNF-α staining (#$P < 0.05$ vs. control group; *$P < 0.05$ vs. vehicle group).

loaded-aspirin could be controllably released from the ASP-Lip@GelMA. The released aspirin can fully cover the inflammatory cycle after intervertebral disc surgery to inhibit inflammatory factor expression and attenuate the release of HMGB1, thereby preventing postoperative recurrence of disc herniation. Thus, ASP-Lip@GelMA could be an effective implant after intervertebral discectomy to prevent postoperative recurrence of disc herniation.

## CRediT authorship contribution statement

**Yu Liu:** Methodology, Investigation, Writing - original draft. **Jiacheng Du:** Conceptualization, Resources, Writing - review & editing. **Peng Peng:** Conceptualization, Resources, Writing - review & editing. **Ruoyu Cheng:** Investigation, Writing - original draft. **Jiayi Lin:** Investigation. **Congxin Xu:** Validation. **Huilin Yang:** Supervision, Writing - review & editing. **Wenguo Cui:** Supervision, Writing - review & editing. **Haiqing Mao:** Supervision, Writing - review & editing. **Yuling Li:** Supervision, Writing - review & editing. **Dechun Geng:** Supervision, Writing - review & editing.

## Declaration of competing interest

The authors declare no conflict of interest.

## Acknowledgments

We thank the financial support of the following funds for our study: National Nature Science Foundation of China (81873991 and 81972104), Natural Science Foundation of Jiangsu Province (BK20180001), a Project Funded by the Priority Academic Program Development of Jiangsu Higher Education Institutions (PAPD) and Application of Key Technology Research Program of Suzhou City (SS201858).

## Appendix A. Supplementary data

Supplementary data to this article can be found online at https://doi.org/10.1016/j.bioactmat.2020.07.008.

## References

[1] N. Maniadakis, A. Gray, The economic burden of back pain in the UK, Pain 84 (2000) 95–103 https://doi:10.1016/s0304-3959(99)00187-6.
[2] B.F. Walker, The prevalence of low back pain: a systematic review of the literature from 1966 to 1998, J. Spinal Disord. 13 (2000) 205–217 https://doi:10.1097/00002517-200006000-00003.
[3] J.W.S. Vlaeyen, C.G. Maher, K. Wiech, J. Van Zundert, C.B. Meloto, L. Diatchenko, M.C. Battie, M. Goossens, B. Koes, S.J. Linton, Low back pain, Nat. Rev. Dis. Prim. 4 (2018) 52 https://doi:10.1038/s41572-018-0052-1.
[4] J.H. Heo, C.H. Kim, C.K. Chung, Y. Choi, Y.G. Seo, D.H. Kim, S.B. Park, J.H. Moon, W. Heo, J.M. Jung, Quantity of disc removal and radiological outcomes of percutaneous endoscopic lumbar discectomy, Pain Physician 20 (2017) E737–E746.
[5] B.J. Shin, Risk factors for recurrent lumbar disc herniations, Asian Spine J. 8 (2014) 211–215 https://doi:10.4184/asj.2014.8.2.211.
[6] M. Dudek, N. Yang, J.P. Ruckshanthi, J. Williams, E. Borysiewicz, P. Wang, A. Adamson, J. Li, J.F. Bateman, M.R. White, R.P. Boot-Handford, J.A. Hoyland, Q.J. Meng, The intervertebral disc contains intrinsic circadian clocks that are regulated by age and cytokines and linked to degeneration, Ann. Rheum. Dis. 76 (2017) 576–584 https://doi:10.1136/annrheumdis-2016-209428.
[7] M. Molinos, C.R. Almeida, J. Caldeira, C. Cunha, R.M. Goncalves, M.A. Barbosa, Inflammation in intervertebral disc degeneration and regeneration, J. R. Soc. Interface 12 (2015) 20150429 https://doi:10.1098/rsif.2015.0429.
[8] A.J. Silva, J.R. Ferreira, C. Cunha, J.V. Corte-Real, M. Bessa-Goncalves,

M.A. Barbosa, S.G. Santos, R.M. Goncalves, Macrophages down-regulate gene expression of intervertebral disc degenerative markers under a pro-inflammatory microenvironment, Front. Immunol. 10 (2019) 1508 https://doi:10.3389/fimmu.2019.01508.
[9] E. Tartour, New therapeutic targets in the inflammatory microenvironment, ESMO Open 3 (2018) e000310 https://doi:10.1136/esmoopen-2017-000310.
[10] G.A. Hasan, R.A. Sheta, H.Q. Raheem, L.M. Al–Naser, The effect of intradiscal vancomycin powder in the prevention of postoperative discitis: RCT study, Interdiscipl. Neurosurg. 21 (2020) 100705 https://doi:10.1016/j.inat.2020.100705.
[11] K. Otoshi, S. Kikuchi, K. Kato, M. Sekiguchi, S. Konno, Anti-HMGB1 neutralization antibody improves pain-related behavior induced by application of autologous nucleus pulposus onto nerve roots in rats, Spine 36 (2011) E692–E698 https://doi:10.1097/BRS.0b013e3181ecd675.
[12] S. Yamada, I. Maruyama, HMGB1, a novel inflammatory cytokine, Clin. Chim. Acta 375 (2007) 36–42 https://doi:10.1016/j.cca.2006.07.019.
[13] S. Roberts, H. Evans, J. Trivedi, J. Menage, Histology and pathology of the human intervertebral disc, J. Bone Joint Surg. Am. 88 (2006) 10–14 https://doi:10.2106/JBJS.F.00019.
[14] G.O. Elhassan, Design and evaluation of controlled release matrix tablet of aspirin by using hydrophobic polymer, Int. J. Pharmaceut. Res. Allied Sci. 6 (2017) 32–41 https://10.1155/2020/8017035.
[15] H.J. Moon, K.H. Choi, D.H. Kim, H.J. Kim, Y.K. Cho, K.H. Lee, J.H. Kim, Y.J. Choi, Effect of lumbar stabilization and dynamic lumbar strengthening exercises in patients with chronic low back pain, Ann. Rehabil. Med. 37 (2013) 110–117 https://doi:10.5535/arm.2013.37.1.110.
[16] W. Wu, Y. Dai, H. Liu, R. Cheng, Q. Ni, T. Ye, W. Cui, Local release of gemcitabine via in situ UV-crosslinked lipid-strengthened hydrogel for inhibiting osteosarcoma, Drug Deliv. 25 (2018) 1642–1651 https://doi:10.1080/10717544.2018.1497105.
[17] X. Zhao, X. Sun, L. Yildirimer, Q. Lang, Z.Y.W. Lin, R. Zheng, Y. Zhang, W. Cui, N. Annabi, A. Khademhosseini, Cell infiltrative hydrogel fibrous scaffolds for accelerated wound healing, Acta Biomater. 49 (2017) 66–77 https://doi:10.1016/j.actbio.2016.11.017.
[18] D. Cao, X. Zhang, M.D. Akabar, Y. Luo, H. Wu, X. Ke, T. Ci, Liposomal doxorubicin loaded PLGA-PEG-PLGA based thermogel for sustained local drug delivery for the treatment of breast cancer, Artif. Cells Nanomed. Biotechnol. 47 (2019) 181–191 https://doi:10.1080/21691401.2018.1548470.
[19] J.S. Seong, M.E. Yun, S.N. Park, Surfactant-stable and pH-sensitive liposomes coated with N-succinyl-chitosan and chitooligosaccharide for delivery of quercetin, Carbohydr. Polym. 181 (2018) 659–667 https://doi:10.1016/j.carbpol.2017.11.098.
[20] X. Mao, R. Cheng, H. Zhang, J. Bae, L. Cheng, L. Zhang, L. Deng, W. Cui, Y. Zhang, H.A. Santos, X. Sun, Self-Healing and injectable hydrogel for matching skin flap regeneration, Adv. Sci. 6 (2019) 1801555 https://doi:10.1002/advs.201801555.
[21] T. Xin, Y. Gu, R. Cheng, J. Tang, Z. Sun, W. Cui, L. Chen, Inorganic strengthened hydrogel membrane as regenerative periosteum, ACS Appl. Mater. Interfaces 9 (2017) 41168–41180 https://doi:10.1021/acsami.7b13167.
[22] C. Feng, Y. Zhang, M. Yang, M. Lan, H. Liu, J. Wang, Y. Zhou, B. Huang, The matrikine N-acetylated proline-glycine-proline induces premature senescence of nucleus pulposus cells via CXCR1-dependent ROS accumulation and DNA damage and reinforces the destructive effect of these cells on homeostasis of intervertebral discs, Biochim. Biophys. Acta (BBA) - Mol. Basis Dis. 1863 (2017) 220–230 https://doi:10.1016/j.bbadis.2016.10.011.
[23] D.N. Paglia, H. Singh, T. Karukonda, H. Drissi, I.L. Moss, PDGF-BB delays degeneration of the intervertebral discs in a rabbit preclinical model, Spine 41 (2016) E449–E458 https://doi:10.1097/BRS.0000000000001336.
[24] X. Xia, J. Guo, F. Lu, J. Jiang, SIRT1 plays a protective role in intervertebral disc degeneration in a puncture-induced rodent model, Spine 40 (2015) E515–E524 https://doi:10.1097/BRS.0000000000000817.
[25] Y. Liu, J. Lin, X. Wu, X. Guo, H. Sun, B. Yu, J. Shen, J. Bai, Z. Chen, H. Yang, D. Geng, H. Mao, Aspirin-mediated attenuation of intervertebral disc degeneration by ameliorating reactive oxygen species in vivo and in vitro, Oxid. Med. Cell. Longev. 6 (2019) 7189854 https://doi:10.1155/2019/7189854.
[26] H.J. Mao, Q.X. Chen, B. Han, F.C. Li, J. Feng, Z.L. Shi, M. Lin, J. Wang, The effect of injection volume on disc degeneration in a rat tail model, Spine 36 (2011) E1062–E1069 https://doi:10.1097/BRS.0b013e3182027d42.
[27] X. Wu, Y. Liu, X. Guo, W. Zhou, L. Wang, J. Shi, Y. Tao, M. Zhu, D. Geng, H. Yang, H. Mao, Prolactin inhibits the progression of intervertebral disc degeneration through inactivation of the NF-kappaB pathway in rats, Cell Death Dis. 9 (2018) 98 https://doi:10.1038/s41419-017-0151-z.
[28] D.S. Lu, Y. Shono, I. Oda, K. Abumi, K. Kaneda, Effects of chondroitinase ABC and chymopapain on spinal motion segment biomechanics. An in vivo biomechanical, radiologic, and histologic canine study, Spine 22 (1997) 1828–1834 discussion 1834-5 https://doi:10.1097/00007632-199708150-00006.
[29] K. Masuda, Y. Aota, C. Muehleman, Y. Imai, M. Okuma, E.J. Thonar, G.B. Andersson, H.S. An, A novel rabbit model of mild, reproducible disc degeneration by an anulus needle puncture: correlation between the degree of disc injury and radiological and histological appearances of disc degeneration, Spine 30 (2005) 5–14 https://doi:10.1097/01.brs.0000148152.04401.20.
[30] R.J. Hlubek, G.M. Mundis Jr., Treatment for recurrent lumbar disc herniation, Curr. Rev. Musculoskelet. Med. 10 (2017) 517–520 https://doi:10.1007/s12178-017-9450-3.
[31] K.T. Kim, S.W. Park, Y.B. Kim, Disc height and segmental motion as risk factors for recurrent lumbar disc herniation, Spine 34 (2009) 2674–2678 https://doi:10.1097/BRS.0b013e3181b4aaac.
[32] G.L. Ambrossi, M.J. McGirt, D.M. Sciubba, T.F. Witham, J.P. Wolinsky, Z.L. Gokaslan, D.M. Long, Recurrent lumbar disc herniation after single-level lumbar discectomy: incidence and health care cost analysis, Neurosurgery 65 (2009) 574–578 https://doi:10.1227/01.NEU.0000350224.36213.F9.
[33] M.F. Shamji, L.A. Setton, W. Jarvis, S. So, J. Chen, L. Jing, R. Bullock, R.E. Isaacs, C. Brown, W.J. Richardson, Proinflammatory cytokine expression profile in degenerated and herniated human intervertebral disc tissues, Arthritis Rheum. 62 (2010) 1974–1982 https://doi:10.1002/art.27444.
[34] J.P. Urban, S. Roberts, Degeneration of the intervertebral disc, Arthritis Res. Ther. 5 (2003) 120–130 https://doi:10.1186/ar629.
[35] C. Weiler, A.G. Nerlich, B.E. Bachmeier, N. Boos, Expression and distribution of tumor necrosis factor alpha in human lumbar intervertebral discs: a study in surgical specimen and autopsy controls, Spine 30 (2005) 44–53 discussion 54 https://doi:10.1097/01.brs.0000149186.63457.20.
[36] H.E. Gruber, G.L. Hoelscher, S. Bethea, J. Ingram, M. Cox, E.N. Hanley Jr., High-mobility group box-1 gene, a potent proinflammatory mediators, is upregulated in more degenerated human discs in vivo and its receptor upregulated by TNF-alpha exposure in vitro, Exp. Mol. Pathol. 98 (2015) 427–430 https://doi:10.1016/j.yexmp.2015.03.001.
[37] E. Venereau, F. De Leo, R. Mezzapelle, G. Careccia, G. Musco, M.E. Bianchi, HMGB1 as biomarker and drug target, Pharmacol. Res. 111 (2016) 534–544 https://doi:10.1016/j.phrs.2016.06.031.
[38] P. Scaffidi, T. Misteli, M.E. Bianchi, Release of chromatin protein HMGB1 by necrotic cells triggers inflammation, Nature 418 (2002) 191–195 https://doi:10.1038/nature00858.
[39] F. Fu, Z. Chen, Z. Zhao, H. Wang, L. Shang, Z. Gu, Y. Zhao, Bio-inspired self-healing structural color hydrogel, Proc. Natl. Acad. Sci. U.S.A. 114 (2017) 5900–5905 https://doi:10.1073/pnas.1703616114.
[40] K. Yue, G. Trujillo-de Santiago, M.M. Alvarez, A. Tamayol, N. Annabi, A. Khademhosseini, Synthesis, properties, and biomedical applications of gelatin methacryloyl (GelMA) hydrogels, Biomaterials 73 (2015) 254–271 https://doi:10.1016/j.biomaterials.2015.08.045.
[41] L. Wang, Y. Wu, T. Hu, P.X. Ma, B. Guo, Aligned conductive core-shell biomimetic scaffolds based on nanofiber yarns/hydrogel for enhanced 3D neurite outgrowth alignment and elongation, Acta Biomater. 96 (2019) 175–187 https://doi:10.1016/j.actbio.2019.06.035.
[42] Y. Wu, L. Wang, B. Guo, P.X. Ma, Interwoven aligned conductive nanofiber yarn/hydrogel composite scaffolds for engineered 3D cardiac anisotropy, ACS Nano 11 (2017) 5646–5659 https://doi:10.1021/acsnano.7b01062.
[43] H.J. Wilke, P. Neef, M. Caimi, T. Hoogland, L.E. Claes, New in vivo measurements of pressures in the intervertebral disc in daily life, Spine 24 (1999) 755–762 https://doi:10.1097/00007632-199904150-00005.
[44] J.E. Frith, A.R. Cameron, D.J. Menzies, P. Ghosh, D.L. Whitehead, S. Gronthos, A.C. Zannettino, J.J. Cooper-White, An injectable hydrogel incorporating mesenchymal precursor cells and pentosan polysulphate for intervertebral disc regeneration, Biomaterials 34 (2013) 9430–9440 https://doi:10.1016/j.biomaterials.2013.08.072.
[45] L.J. Smith, D.J. Gorth, B.L. Showalter, J.A. Chiaro, E.E. Beattie, D.M. Elliott, R.L. Mauck, W. Chen, N.R. Malhotra, In vitro characterization of a stem-cell-seeded triple-interpenetrating-network hydrogel for functional regeneration of the nucleus pulposus, Tissue Eng. A 20 (2014) 1841–1849 https://doi:10.1089/ten.TEA.2013.0516.
[46] J.D. Thomas, G. Fussell, S. Sarkar, A.M. Lowman, M. Marcolongo, Synthesis and recovery characteristics of branched and grafted PNIPAAm-PEG hydrogels for the development of an injectable load-bearing nucleus pulposus replacement, Acta Biomater. 6 (2010) 1319–1328 https://doi:10.1016/j.actbio.2009.10.024.
[47] J.M. Cloyd, N.R. Malhotra, L. Weng, W. Chen, R.L. Mauck, D.M. Elliott, Material properties in unconfined compression of human nucleus pulposus, injectable hyaluronic acid-based hydrogels and tissue engineering scaffolds, Eur. Spine J. 16 (2007) 1892–1928 https://doi:10.1007/s00586-007-0443-6.
[48] J.C. Iatridis, L.A. Setton, M. Weidenbaum, V.C. Mow, The viscoelastic behavior of the non-degenerate human lumbar nucleus pulposus in shear, J. Biomech. 30 (1997) 1005–1013 https://doi:10.1016/s0021-9290(97)00069-9.
[49] Y.X. Liu, Q. Huang, J. Wang, F.F. Fu, J.N. Ren, Y.J. Zhao, Microfluidic generation of egg-derived protein microcarriers for 3D cell culture and drug delivery, Sci. Bull. 62 (2017) 1283–1290 https://doi:10.1016/j.scib.2017.09.006.